



Uncertainty Quantification of the 1-D SFR Thermal Stratification Model via the Latin Hypercube Sampling Monte Carlo Method

Cihang Lu & Zeyun Wu

To cite this article: Cihang Lu & Zeyun Wu (2022) Uncertainty Quantification of the 1-D SFR Thermal Stratification Model via the Latin Hypercube Sampling Monte Carlo Method, Nuclear Technology, 208:1, 37-48, DOI: [10.1080/00295450.2021.1874779](https://doi.org/10.1080/00295450.2021.1874779)

To link to this article: <https://doi.org/10.1080/00295450.2021.1874779>



Published online: 13 Apr 2021.



Submit your article to this journal [↗](#)



Article views: 89



View related articles [↗](#)



View Crossmark data [↗](#)



Uncertainty Quantification of the 1-D SFR Thermal Stratification Model via the Latin Hypercube Sampling Monte Carlo Method

Cihang Lu^{id} and Zeyun Wu^{id}*

Virginia Commonwealth University, Department of Mechanical and Nuclear Engineering, 401 W. Main Street, Richmond, Virginia 23219

Received November 2, 2020

Accepted for Publication January 7, 2021

Abstract — A one-dimensional (1-D) thermal stratification (TS) model was recently developed in our research group to predict the TS phenomenon in pool-type sodium-cooled fast reactors. This paper performs uncertainty quantification (UQ) of the 1-D TS model to evaluate its performance by considering the aleatoric uncertainties that existed in the model parameters and to identify the plausible sources of the epistemic uncertainties. The Latin hypercube sampling–Monte Carlo method (LHS-MC), which is elaborated with an example in this paper to facilitate its understanding and implementation, is used for the UQ process. The advantages of LHS-MC, including both better stability and better accuracy than the conventional random sampling–Monte Carlo method with fewer realizations, are demonstrated in this paper.

In total, 648 temperature measurements acquired from nine experimental transients performed in a university-scale Thermal Stratification Experimental Facility are used to evaluate the performance of the computational 1-D TS model. The UQ result shows that 77.5% of the experimental data can be predicted by the 1-D TS model within uncertainty ranges, which indicates the good performance of the computational model when the aleatoric uncertainties are correctly captured. The rest 22.5% of the experimental data are found located outside of the uncertainty ranges, which reveals the existence of the epistemic uncertainties caused by the lack of understanding of the TS phenomenon and defects in the 1-D model. The simple jet model currently employed by the 1-D TS model is thought to be one of the attributors to these defects.

Keywords — Uncertainty quantification, Latin hypercube sampling Monte Carlo, thermal stratification, sodium-cooled fast reactor.

Note — Some figures may be in color only in the electronic version.

I. INTRODUCTION

In nuclear engineering, thermal stratification (TS) phenomenon refers to the phenomenon where stratified layers of coolant with a large temperature gradient are formed in different components of nuclear systems.¹ This phenomenon can take place in different reactor types and further lead to uncertainties in reactor safety. In order to prevent its formation or to mitigate the damage it causes, computational efforts with different fidelities have been made to predict the occurrence of TS. System-level codes usually rely on zero-dimensional models to provide fast

yet approximated solutions for simple cases at low computational cost, while three-dimensional computational fluid dynamics (CFD) modeling can give more accurate calculations but are computationally expensive.²

In this regard, efforts were made by our research group to establish a fast-running, one-dimensional (1-D) TS model to provide reliable TS predictions in the upper plenum of pool-type sodium-cooled fast reactors (SFRs). A preliminary 1-D TS model was built following the work of Peterson,³ and its performance was evaluated by using experimental data acquired from the Thermal Stratification Experimental Facility (TSTF) developed at the University of Wisconsin–Madison.⁴ The preliminary 1-D TS model was able to finish the calculation within

*E-mail: zwu@vcu.edu

seconds by using a single processor core, and achieved similar performance with CFD calculations in terms of the prediction of TS for the designated cases studied at the TSTF (Ref. 5). However, nonnegligible discrepancies between the 1-D predictions and the experimental measurements of the temperature were observed because static thermal conductivity of sodium was employed in the preliminary 1-D TS model, while heat transfer was actually enhanced by the flow turbulence created during the TS procedure. Improvements were therefore made to the preliminary 1-D model in a follow-up work by correlating the effective thermal conductivity to the static one considering the turbulent heat conduction effect. The coefficients of the correlation were determined by a Bayesian-based inverse uncertainty quantification (UQ) method, and the performance of the 1-D TS model has been demonstrated to be improved compared to that of the preliminary version. The enhanced 1-D model was detailed in Ref. 6.

The objective of this paper is to perform a UQ study on the current 1-D TS model to achieve a more quantitative evaluation of the model performance and to identify the plausible existing defects. Sampling-based stochastic UQ approaches were employed in the study. Among them, the straightforward random sampling–Monte Carlo method (RS-MC) was used to provide a reference uncertainty calculation, while the advanced Latin hypercube sampling–Monte Carlo method⁷ (LHS-MC), which is theoretically more efficient and stable than RS-MC, was employed to quantify the uncertainties associated with temperature predictions of the 1-D TS model.

The rest of this paper is organized as follows: Sec. II briefly discusses the development of the 1-D TS model. The experiments, from which the data used for the 1-D TS model performance evaluation were acquired, are also briefly described in Sec. II. Section III introduces both sampling-based stochastic approaches used in this work for UQ. The advantages of LHS-MC will be demonstrated by giving an example. Section IV shows the results obtained from the UQ study on the 1-D TS model. Section V concludes the paper by summarizing the UQ work performed and providing a general discussion on stochastic UQ methods.

II. DEVELOPMENT OF THE TS MODEL

This section briefly presents the parameters, coefficients, and models employed in the 1-D TS model, which are important for the UQ. The acquisition of the experimental data, which are used in this work for the

performance evaluation of the 1-D TS model, is also briefly introduced in the first part of the section for completeness. The experimental configuration and the flow conditions considered in different transients are described. Both the development of the 1-D TS model and the descriptions of the experimental settings have been documented in detail in our previous publications.^{5,6} Information that is important for the UQ conducted is summarized in this section so that readers can understand this work without referring to numerous references.

II.A. Experimental Configuration and Conditions

Experiments were performed in the TSTF that was built at the University of Wisconsin–Madison.⁴ The TSTF has a cylindrical test section with a diameter of about 30 cm and a height of about 130 cm. During experimental transients, the test section was initially filled with sodium at a certain temperature; sodium jets at 200°C were then injected from the inlet located at the bottom of the test section. The outlet was located about 83 cm higher than the inlet, as shown in Fig. 1. A cylindrical upper instrumentation structure (UIS) can be installed in the test section to emulate the in-vessel components located in the upper plenum of an SFR. When it was installed, the bottom of the UIS was about 5 cm from the jet inlet. Nine experiments, consisting of different jet volumetric flow rates and initial temperatures in the test section, were performed. Among these nine experiments, three were performed with the UIS installed in the test section, and six were performed without the UIS, as summarized in Table I. The temperature of the ambient fluid was continuously measured during the nine experiments with thermocouples (TCs) installed in the test section at 2.54 cm (1 in.) from its wall at four different axial locations, namely 16.5, 27.9, 55.9, and 69.9 cm above the inlet. At each of the four axial locations, temperature was measured simultaneously by two different TCs. The names of the TCs and their axial locations are indicated in Fig. 1. The jet volumetric flow rate measurement had an uncertainty of 3%, while the temperature measurement had an uncertainty of 1% (Ref. 8).

II.B. Computational 1-D TS Model

Following the work of Peterson,³ the 1-D TS model was developed to predict the TS phenomenon in the upper plenum of pool-type SFRs. The 1-D TS model was developed by combining the equations of conservation of mass and energy, and by using integral techniques to convert the jets to source terms in the diffusion

TABLE I
Flow Conditions of the Nine Experiments*

Configuration	Test	Inlet Temperature (°C)	Initial Temperature (°C)	Flow Rate (L/s)
With UIS	1	200	250	6
	2	200	250	10
	3	200	225	10
Without UIS	4	200	300	1.5
	5	200	250	3
	6	200	300	3
	7	200	250	3.7
	8	200	300	10
	9	200	250	10

*Reference 6.

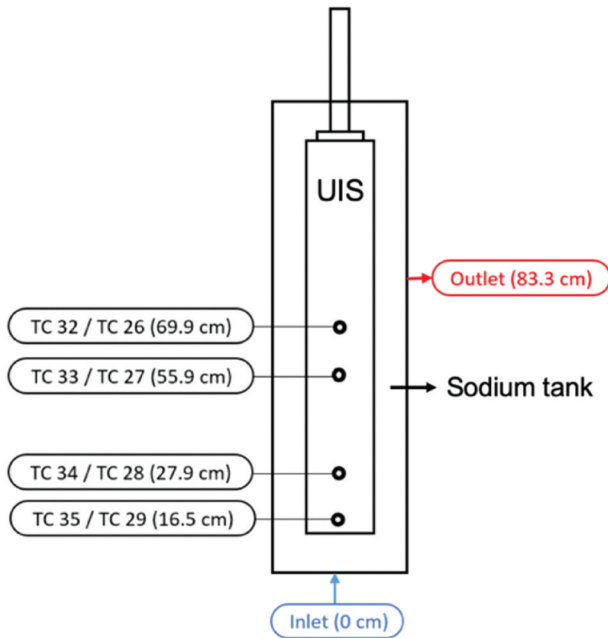


Fig. 1. Schematic of the test section of the TSTF (Ref. 6).

$c_{p,amb}$ = heat capacity of ambient fluid

T_{amb} = temperature of ambient fluid

A_{amb} = cross-sectional area of ambient fluid

$k_{eff,amb}$ = effective thermal conductivity of ambient fluid

Q_{jet} = volumetric flow rate of impinging jet

$c_{p,jet}$ = heat capacity of impinging jet

ρ_{jet} = mass density of impinging jet

T_{jet} = temperature of impinging jet

Q'_{jet} = linear volumetric dispersion rate of the impinging jet.

During the experiments, turbulence was caused by the dispersion of the impinging jets and further enhanced the heat transfer of the ambient fluid. The effective thermal conductivity of the ambient fluid $k_{eff,amb}$ was therefore different from the static thermal conductivity $k_{s,amb}$ of sodium. The ratio of the turbulent Reynolds number Re_{τ} to the Richardson number Ri was used to correlate $k_{eff,amb}$ with $k_{s,amb}$ by using the similar form as that established by Shih et al.,⁹ as shown in Eq. (2):

$$k_{eff,amb} = m \left(\frac{Re_{\tau}}{Ri} \right)^p \cdot k_{s,amb} \quad (2)$$

convection equation.⁵ The analytical form of the 1-D TS model is shown in Eq. (1):

$$\rho_{amb} c_{p,amb} \frac{\partial T_{amb}}{\partial t} + \rho_{amb} c_{p,amb} \frac{Q_{jet}}{A_{amb}} \frac{\partial T_{amb}}{\partial z} - \frac{\partial}{\partial z} \left(k_{eff,amb} \frac{\partial T_{amb}}{\partial z} \right) = \frac{c_{p,jet} \rho_{jet}}{A_{amb}} Q'_{jet} (T_{jet} - T_{amb}) \quad (1)$$

where

ρ_{amb} = mass density of ambient fluid

The coefficients m and p , which minimized the mismatches between the predictions and experimental measurements, were determined by using a data assimilation process: the inverse uncertainty quantification (inverse UQ) method.⁶ Thanks to the advantage of the inverse UQ method,^{10,11} the uncertainties associated with the coefficients were quantified at the same time. Experimental data

acquired in tests 1, 2, 5, and 6 were used during the inverse UQ process. According to the different values of Re_c/Ri of the experiments, p was found to follow a probability density function (PDF) of $N(0.33, 0.0025)$ for tests 1, 2, and 3, and a PDF of $N(0.13, 0.017)$ for tests 4 through 9. Because m and p were generated in pairs, an m was determined corresponding to each value of p during the inverse UQ process. We considered the standard deviations of p as its associated uncertainties, and further used them to determine the uncertainties of the 1-D temperature prediction in this work.

A simple model was employed to calculate Q'_{jet} . It was assumed that the impinging jets uniformly dispersed in the ambient fluid within a length of L_{jet} , and Q'_{jet} was correlated to Q_{jet} by Eq. (3):

$$Q'_{jet} = Q_{jet}/L_{jet} \quad (3)$$

In tests 1, 2, and 3, where the UIS was installed in the test section, the impinging jets were blocked by the UIS after entering the test section and were unable to rise above the UIS before dispersing in the ambient fluid. L_{jet} was therefore considered equal to the distance between the bottom of the UIS and the jet inlet surface, $Z_{UIS} = 5$ cm. In tests 4 through 9, where the UIS was absent, the change in jet velocity was correlated with the standard acceleration due to gravity g_0 and time t , as shown in Eq. (4):

$$dv_{jet} = - \left(C \frac{v_{jet}^2 \rho_{amb}}{\rho_{jet}} + \frac{\rho_{jet} - \rho_{amb}}{\rho_{jet}} g_0 \right) dt \quad (4)$$

L_{jet} was then calculated by integrating jet velocity. The coefficient C in Eq. (4) was determined to be 4.3 by using the experimental measurements of tests 5 and 6 through the use of a data assimilation method.⁵ We did not consider the uncertainties of the 1-D temperature prediction caused by the jet model in this work because the uncertainties of C were unknown.

The thermal properties of sodium were calculated by referring to the work in Ref. 12, which suggested that the estimated $C_{p,amb}$ had an uncertainty of 3%, and the estimated $k_{s,amb}$ had an uncertainty of 5%.

III. UNCERTAINTY QUANTIFICATION METHOD

Two sampling-based stochastic UQ approaches, namely the RS-MC and the LHS-MC, were employed in this work. The RS-MC method is discussed in Sec. III.A, and the LHS-MC method is illustrated in Sec. III.B. For

comparison, the UQ results obtained from the RS-MC method with a large number of samples are used as reference solutions in the current work.

III.A. RS-MC Method

We assumed that the uncertainties in the predicted temperature were caused by the uncertainty propagation of five parameters, including jet volumetric flow rate Q_{jet} , jet temperature T_{jet} , heat capacity of the ambient fluid $C_{p,amb}$, static thermal conductivity of the ambient fluid $k_{s,amb}$, and coefficient p , which correlates the effective thermal conductivity of the ambient fluid $k_{eff,amb}$ with the static thermal conductivity $k_{s,amb}$. The jet volumetric flow rate measurement was considered to have an uncertainty of 3%, and an uncertainty of 1% was attributed to the temperature measurement of both jet and ambient fluid, as introduced in Sec. II.A. The uncertainties of $C_{p,amb}$ and $k_{s,amb}$ were considered to be 3% and 5%, respectively, while the uncertainties associated with coefficient p were determined during the inverse UQ process, as introduced in Sec. II.B.

We conducted UQ with the RS-MC method first, the process of which was rather straightforward. Experimental measurements were considered to follow normal distributions, with a standard deviation equal to the measurement uncertainty and a mean equal to the nominal measured value. The PDFs used in the UQ process are summarized in Table II. We employed 1 000 000 RS-MC realizations because according to our knowledge, this amount of realizations is usually more than enough for both good stability and good accuracy. The convergence of the UQ calculation with 1 000 000 RS-MC realizations can be further demonstrated clearly by Fig. 4 (see Sec. III.B). In each realization, the temperature of the ambient fluid was calculated at the four axial locations by randomly generating the parameters of interest following their PDF. The standard

TABLE II
PDFs of the Five Parameters of Interest

Parameter	PDF	Mean	Standard Deviation
Q_{jet}	Normal	Nominal	3%
T_{jet}	Normal	Nominal	1%
$C_{p,amb}$	Normal	Nominal	3%
$k_{s,amb}$	Normal	Nominal	5%
p (test 1, 2, and 3)	Normal	0.33	0.05
p (test 4 through 9)	Normal	0.13	0.13

deviations of the temperature calculated from all the realizations were considered as the uncertainties of the predicted temperature.

III.B. LHS-MC Method

In order to improve the sampling efficiency in the Monte Carlo method, we employed LHS-MC instead of RS-MC for UQ. LHS is a statistical method for generating near-random samples from multidimensional distributions. LHS was first proposed by McKay and coauthors in 1979 (Ref. 7), and has been widely used in computer experiments¹³ and UQs^{14,15} since then. While the detailed theory of LHS has been introduced in the literature,^{7,13,14,16} its philosophy can be understood as follows: When sampling N combinations of M variables with LHS, the range of each variable is divided into N equal-probable subdivisions. Then N sample points are placed such that each axis-aligned hyperplane contains one (and only one) sample.

Latin hypercube sampling is therefore considered as pseudorandom because the samples are generated by reproducible algorithmic processes rather than in a truly random manner.¹⁴ An example is given in this paragraph to facilitate the understanding of LHS. Assuming that we have three independent variables, x , y , and z , that all follow an identical triangular distribution with a lower limit of 0, a peaking location of 1, and an upper limit of 2, and we would like to generate five sets of samples. The PDF and the cumulative distribution function (CDF) of the variables are shown in Fig. 2. Following the LHS methodology, the range of each variable was divided into five equal-probable subdivisions, namely, $(0, \sqrt{0.4})$, $(\sqrt{0.4}, \sqrt{0.8})$, $(\sqrt{0.8}, 2 - \sqrt{0.8})$, $(2 - \sqrt{0.8}, 2 - \sqrt{0.4})$, and $(2 - \sqrt{0.4}, 2)$. The

subdivisions are separated by vertical straight dashed lines in Fig. 2. In LHS, one sample was randomly placed in each subdivision, and one set of samples was formed by randomly picking one sample for each of the three variables, while each sample can be picked only once.

An example of the five sets of samples generated by using LHS is given in Table III. It is pointed out that although LHS generates multivariable samples by reproducible algorithmic processes rather than in a truly random manner, this method is still “random” to a large extent because (1) the samples are placed in each subdivision stochastically following the probability distribution of the variable and (2) the combination of the samples is made randomly. For the example considered, as samples were made from three variables, there were 14 400 (calculated from $P_5^3 \times P_5^3$) possible combinations of the five sets of samples, and the one shown in Table III was made randomly. LHS is considered to have a “memory” because all the samples must be placed simultaneously in accordance to the others. On the contrary, RS is considered to have no “memories” because the samples of all the variables are placed randomly and independently. An example of the five sets of samples generated by using RS is given in Table III for comparison.

The advantageous characteristic of LHS that each axis-aligned hyperplane contains one (and only one) sample can be graphically interpreted by comparing the five sets of samples generated by both methods. In Fig. 3, samples are marked by dots, and the projections of the subdivisions containing the samples on the three coordinate planes are highlighted with subplanes that clearly demonstrate the characteristic of LHS. The samples generated by LHS therefore have a better capability to cover the whole multivariable sample space with

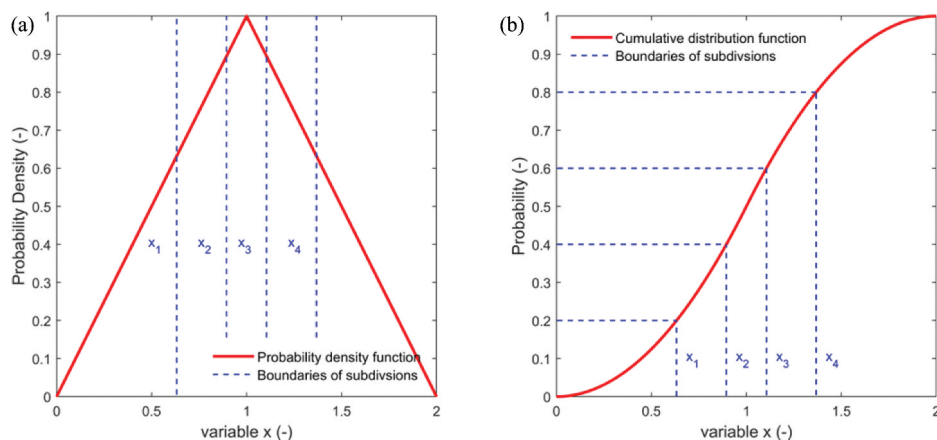


Fig. 2. (a) PDF and (b) CDF of each random variable.

TABLE III
Comparison of the Five Sets of Samples Generated by LHS and RS

	Variable	Sample 1	Sample 2	Sample 3	Sample 4	Sample 5
LHS	x	0.50	0.75	1.05	1.14	1.57
	y	0.27	0.87	0.99	1.24	1.72
	z	0.55	0.71	1.01	1.22	1.71
RS	(x, y, z)	(1.05, 0.99, 1.01)	(1.14, 1.24, 0.55)	(0.50, 0.87, 1.71)	(0.75, 1.72, 0.71)	(1.57, 0.27, 1.22)
	(x, y, z)	(0.84, 0.76, 0.39)	(1.42, 1.30, 0.33)	(1.09, 1.30, 1.03)	(1.05, 0.87, 1.34)	(1.59, 1.07, 1.64)

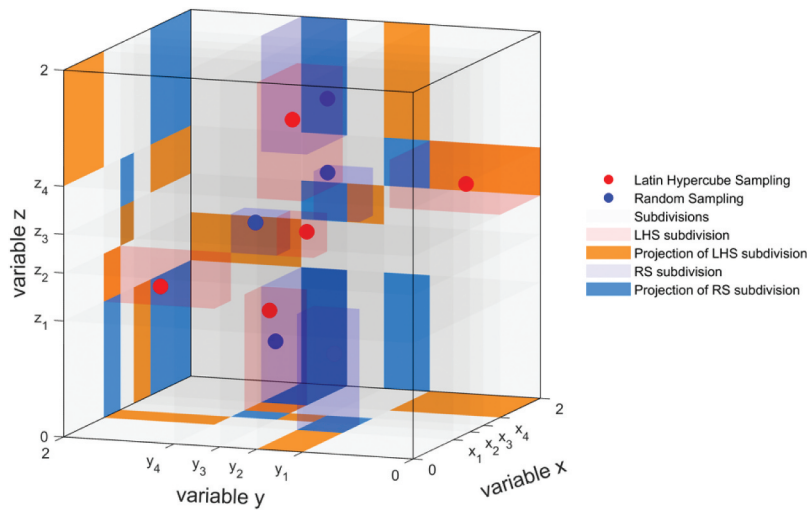


Fig. 3. Comparison of the samples generated by LHS and RS.

fewer samples, which makes LHS-MC theoretically more efficient than RS-MC when the number of samples is small. Other advantages of LHS, including better descriptions of the mean and the population distribution functions, reduced variances, etc., were well discussed in the work of Khan and coworkers.¹⁷

Performing UQ by using 1 000 000 realizations was computationally expensive and surpassed the capability of a common personal computer in this work, as repetitive calculations were needed for all the experimental transients. On the other hand, a decrease in the number of realizations deteriorates both the stability and accuracy of the uncertainty calculation. Therefore, we determined the minimum number of LHS-MC realizations required in order to decrease computational cost while keeping both good stability and good accuracy of the uncertainties calculated. We considered the RS-MC calculation performed for experimental transient test 1 with 1 000 000 realizations as the reference calculation to evaluate the performance of the LHS-MC calculation with fewer realizations because of the truly random

nature of RS-MC and the huge amount of realizations employed. We varied the number of LHS-MC realizations and calculated the maximum error in the uncertainties obtained at all four axial locations throughout test 1. Considering the instability of the RS-MC method, which was more significant when the number of realizations was small, we performed ten LHS-MC calculations for each number of realizations used. The mean values of the errors and the ranges of the errors of the ten LHS-MC runs are shown in Fig. 4 as a function of the number of realizations employed. The performance of the RS-MC is shown in Fig. 4 for comparison.

Figure 4 suggests that the stability and accuracy of both methods increased with a larger number of realizations, while the performance of the LHS-MC was always superior for all the numbers of realizations investigated. We therefore employed the LHS-MC in this work for its better performance. All the results of the UQ presented in Sec. IV were calculated by using the LHS-MC with 200 realizations by considering a maximum error of around 5% in the calculated uncertainty to be acceptable (2000

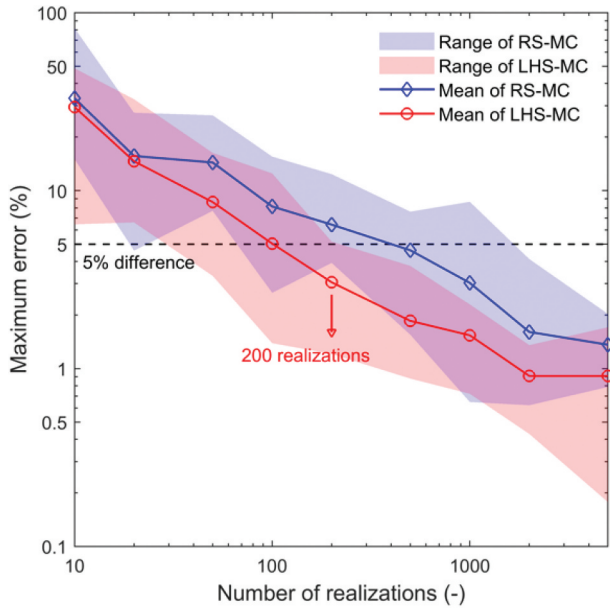


Fig. 4. Comparison of the performance of the LHS-MC and the RS-MC.

realizations were needed if the RS-MC was to be used). Note that the LHS samples used in this work were generated by using the `lhsnorm` function in MATLAB®.

IV. RESULTS AND DISCUSSIONS

We examined the uncertainties of the 1-D temperature prediction for the nine experimental transients using the LHS-MC with 200 realizations for each test. The nominal 1-D TS model prediction of the sodium temperature transient in test 1, together with the associated uncertainties, is

plotted in Fig. 5. The experimental data are also included for comparison. During test 1 transient, the test section was initially filled with sodium at 250°C. A sodium jet with a temperature of 200°C was injected from the bottom of the test section at the beginning of the transient. The temperature of the ambient fluid at TC 29/35 and TC 28/34 (lower positions in the test section, see Fig. 1) first started to decrease due to the entering of the sodium jet with a lower temperature, the temperature at TC 27/33 and TC 26/32 (higher positions in the test section, see Fig. 1) then followed. At about 300 s elapsed time, the temperature of the ambient fluid converged to the temperature of the impinging jet. We selected the temperature measurements at 11 specific elapsed times that cover the whole transient to evaluate the performance of the 1-D TS model. In total, 88 data points were used for the evaluation because temperature was measured twice at each of the four axial locations, as described in Sec. II.A. As shown in Fig. 5, the 1-D TS model was able to predict 77 data points within the range of uncertainties, which made its percentage correctness rate 87.5% for test 1. Comparisons between experimental data and 1-D computational predictions of the sodium temperature with associated uncertainties for tests 2 through 9 are shown in Figs. 6 through 13, respectively. Table IV summarizes the percentage correctness rate of the 1-D TS model for all nine experimental transients.

On average, the 1-D TS model can predict 77.5% of the temperature measurements of the nine experimental transients within the range of uncertainties, which indicates the good capability of the 1-D TS model to predict the TS phenomenon when the aleatoric uncertainties caused by the statistical nature of all physical events are correctly captured. The performance of the 1-D TS model

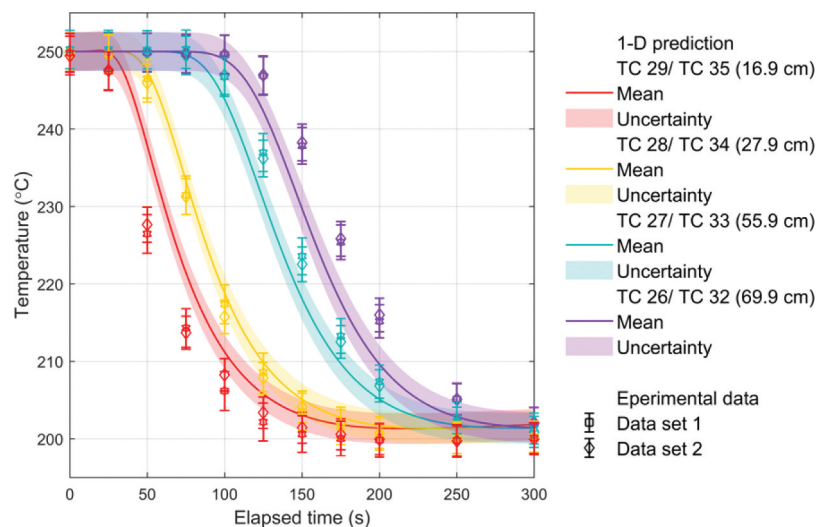


Fig. 5. Experimental and computational predictions with associated uncertainties for sodium temperatures in test 1.

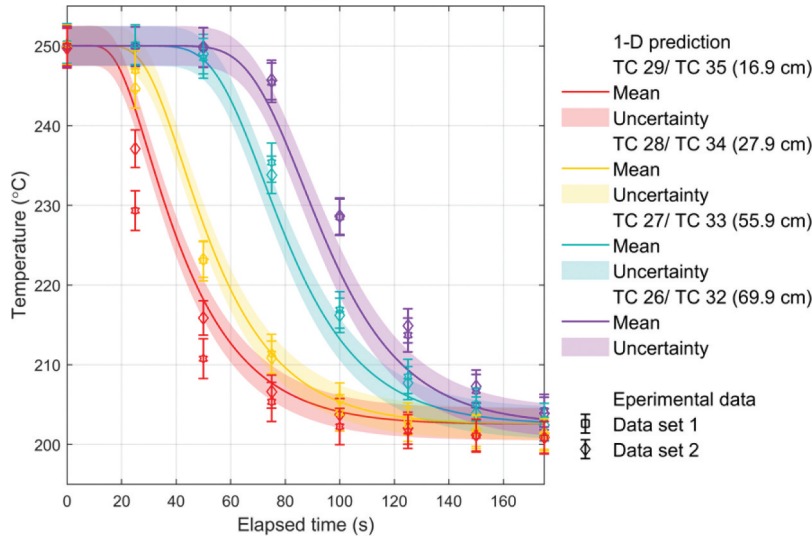


Fig. 6. Experimental and computational predictions with associated uncertainties for sodium temperatures in test 2.

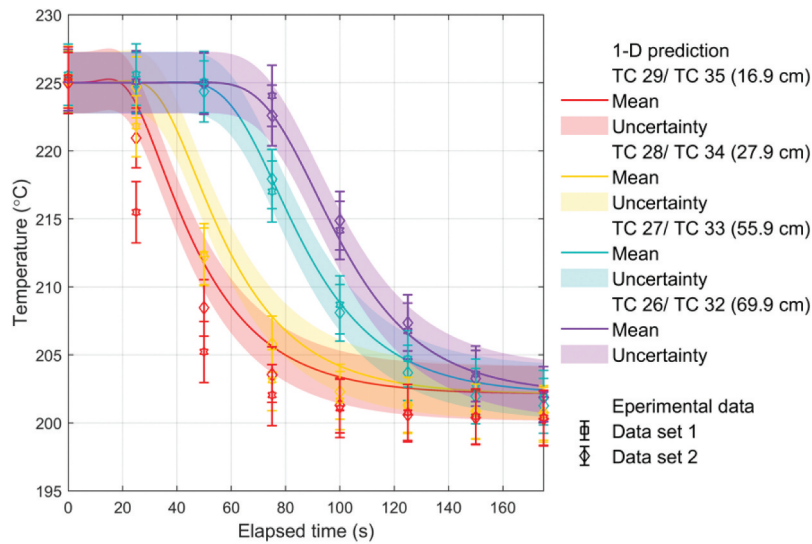


Fig. 7. Experimental and computational predictions with associated uncertainties for sodium temperatures in test 3.

is expected to become more convincing when more experimental data become available for its evaluation. It is pointed out that measurement uncertainties are usually categorized as epistemic if there is the possibility of considering alternative methods of measurement.¹⁸ However, the uncertainties in Q_{jet} , T_{jet} , $C_{p,amb}$, and $k_{s,amb}$ were considered aleatoric in this work because we cannot reduce them by modifying the 1-D TS model.

The 1-D TS model should theoretically have had the best performance when it was applied to tests 1, 2, 5, and 6 because the temperature measurements of these four experimental transients were used during its development by using

data assimilation methods. However, none of these four transients had a percentage correctness rate of 100%. This revealed the existence of another type of uncertainties of the 1-D TS model, which is known as epistemic uncertainties.¹⁸ This type of uncertainties is attributed to the lack of understanding of the physical phenomena or defects in the physics model, etc., and is relatively more difficult to quantify and normally requires more in-depth knowledge to reduce.

In tests 8 and 9, which had the largest jet volumetric flow rates among the nine experimental transients, the measured temperatures at the four axial locations were within the uncertainty range of each other throughout the

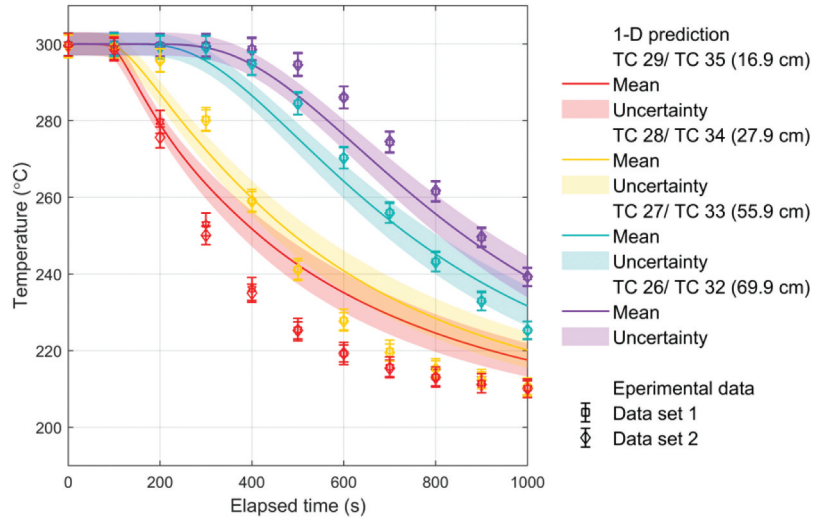


Fig. 8. Experimental and computational predictions with associated uncertainties for sodium temperatures in test 4.

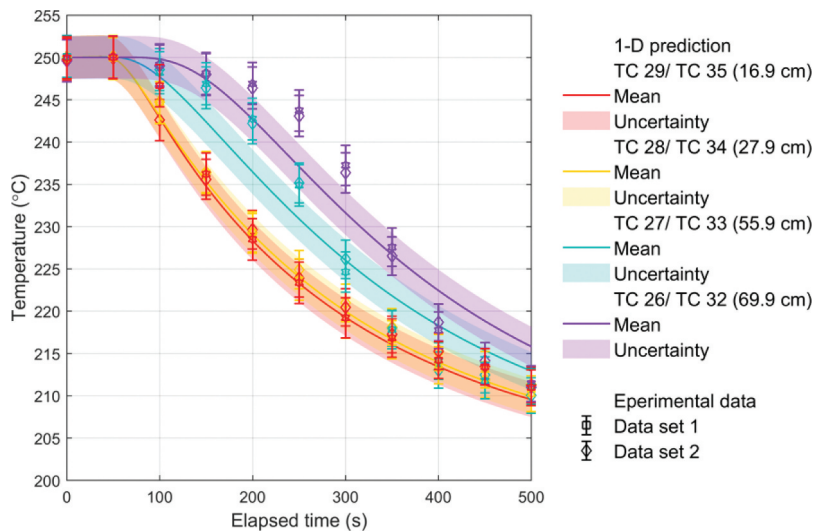


Fig. 9. Experimental and computational predictions with associated uncertainties for sodium temperatures in test 5.

transient. This suggested that the ambient fluid in the tank became turbulent and well mixed due to the large jet injection velocity. The heat transfer of the ambient fluid through heat conduction therefore decreased, and the temperature change of the ambient fluid was mainly caused by the dispersion of the impinging jet. A good jet model became vital for an accurate temperature prediction in this case. The worst performance of the 1-D TS model, when applied to tests 8 and 9, suggested that the simple jet model currently employed in the 1-D TS model should be one of the attributors of the defects in the physics model. Therefore, developing a better jet model will be the focus of our future work in order to decrease the epistemic uncertainties of the 1-D TS model.

V. SUMMARY AND CONCLUSIONS

In this work, we quantified the uncertainties associated with the temperature predictions of the 1-D TS model by using the LHS-MC method. The 1-D TS model was previously developed in our research group to predict the formation of TS in the upper plenum of an SFR during transients. We employed 200 LHS-MC realizations, such that the maximum error of the calculated uncertainty was around 5%.

Sampling-based stochastic UQ approaches are straightforward and easy to implement. They are capable of achieving any desired accuracy when enough realizations are used. Both of these advantages have been

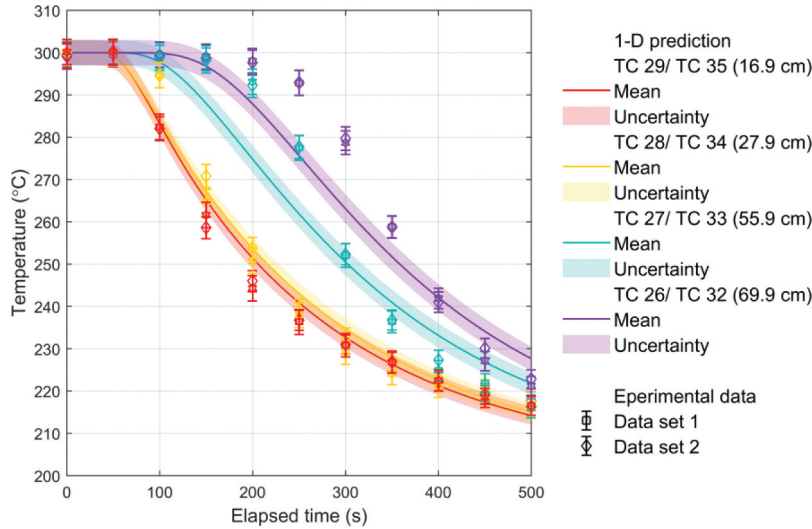


Fig. 10. Experimental and computational predictions with associated uncertainties for sodium temperatures in test 6.

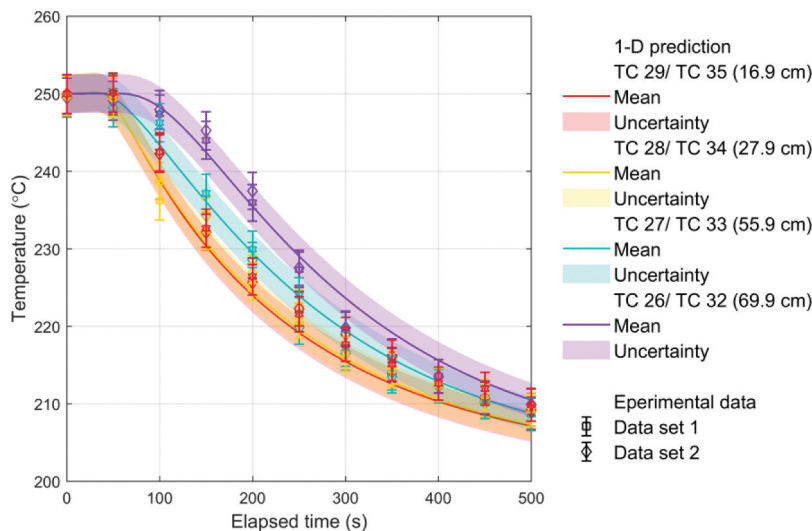


Fig. 11. Experimental and computational predictions with associated uncertainties for sodium temperatures in test 7.

demonstrated in this paper. However, the sampling-based stochastic UQ approaches have the disadvantage of being computationally expensive. Uncertainties can also be calculated through the deterministic UQ approach, the computational cost of which is negligible once the sensitivities of the input parameters are known.¹⁹ We proved in one of our previous publications that the sensitivities of the 1-D–predicted temperature to all the input parameters can be calculated through the discrete adjoint method at the cost of solving the 1-D TS model only twice.²⁰ In this regard, sampling-based stochastic UQ approaches can be hundreds of times more computationally costly compared to the deterministic UQ method.

However, it is well known that deterministic UQ methods are problem specific and not easily generalized. The implementation efforts of the deterministic UQ method for a particular problem could be considerably larger than that of the sampling-based stochastic UQ method.

We evaluated the performance of the 1-D TS model by using experimental data acquired from the TSTF, which was built at the University of Wisconsin–Madison. We considered 648 temperature measurements from nine experimental transients and found that the 1-D TS model can predict 77.5% of the data points within the range of uncertainties. This demonstrated the good capability of the 1-D TS model to provide predictions for the TS

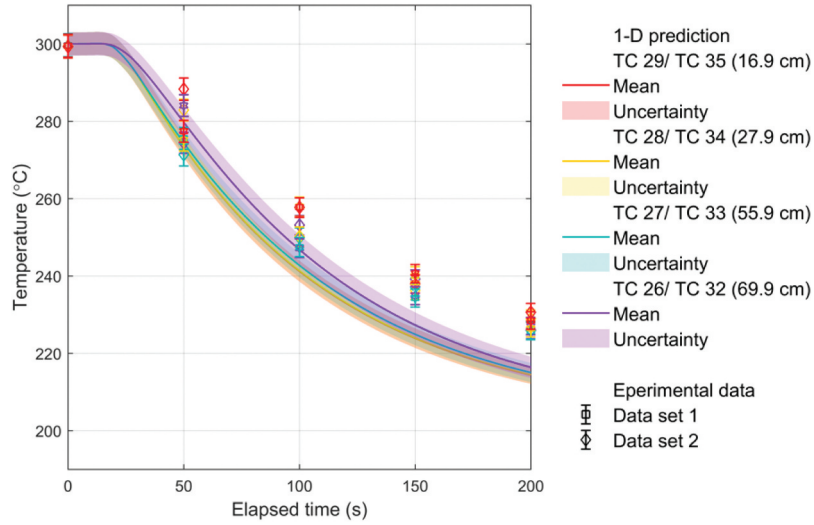


Fig. 12. Experimental and computational predictions with associated uncertainties for sodium temperatures in test 8.

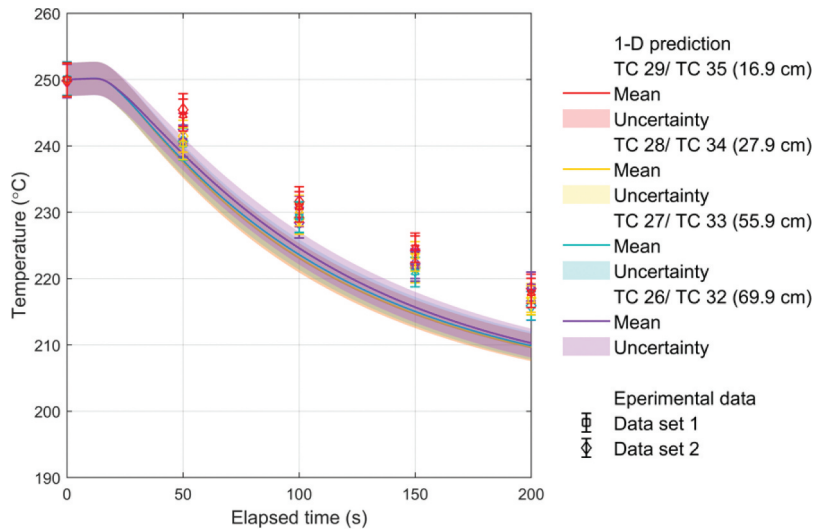


Fig. 13. Experimental and computational predictions with associated uncertainties for sodium temperatures in test 9.

TABLE IV

Performance of 1-D TS Model for the Nine Experimental Transients

Test	Data Points Considered	Data Points Correctly Predicted	Percentage Correctness Rate
1	88	77	87.5%
2	64	58	90.6%
3	64	60	93.8%
4	88	46	52.3%
5	88	77	87.5%
6	88	65	73.9%
7	88	88	100.0%
8	40	16	40.0%
9	40	15	37.5%

phenomenon when the aleatoric uncertainties are correctly captured. However, the temperature predictions cannot reach a percentage correctness rate of 100% even in case where the 1-D TS model was applied to the transients whose experimental data were used for the development of the 1-D TS model through data assimilation methods. This revealed the existence of the epistemic uncertainties, which are caused by the lack of understanding of the TS phenomenon and defects in the 1-D TS model. The fact that the 1-D TS model had the worst performance when it was applied to the experimental transients with the largest impinging jet volumetric flow rate suggested that the simple jet model currently employed in the 1-D TS model is one of the attributors of the defects in the model. Therefore, we will focus on developing a better jet model in our future

work to decrease the epistemic uncertainties and to improve the performance of the 1-D TS model.

Acknowledgments

We thank Dr. Mark Anderson and his research team at the University of Wisconsin–Madison for providing the TSTF experimental data for the evaluation of the 1-D TS model in this paper. We also acknowledge the U.S. Department of Energy Nuclear Energy University Program for the support of our earlier research pertaining to this work.

ORCID

Cihang Lu  <http://orcid.org/0000-0002-6385-6338>

Zeyun Wu  <http://orcid.org/0000-0002-6114-0352>

References

1. T. G. THEOFANOUS et al., “Decay of Buoyancy Driven Stratified Layers with Applications to Pressurized Thermal Shock,” NUREG/CR-3700, US Nuclear Regulatory Commission (May 1984).
2. Z. WU et al., “A Status Review on the Thermal Stratification Modeling Methods for Sodium-Cooled Fast Reactors,” *Prog. Nucl. Energy*, **125**, 103369, (2020); <https://doi.org/10.1016/j.pnucene.2020.103369>.
3. P. F. PETERSON, “Scaling and Analysis of Mixing in Large Stratified Volumes,” *Int. J. Heat Mass Tran.*, **37**, 97 (1994); [https://doi.org/10.1016/0017-9310\(94\)90013-2](https://doi.org/10.1016/0017-9310(94)90013-2).
4. J. SCHNEIDER et al., “Thermal Stratification Analysis for Sodium Fast Reactors,” *Proc. Int. Congress on Advances in Nuclear Power Plants (ICAPP)*, Charlotte, North Carolina, April 9–11, 2018; <https://www.osti.gov/servlets/purl/1435133>.
5. C. LU et al., “An Efficient 1-D Thermal Stratification Model for Pool-Type Sodium-Cooled Fast Reactors,” *Nucl. Technol.*, **206**, 10, 1465 (2020); <https://doi.org/10.1080/00295450.2020.1719799>.
6. C. LU, Z. WU, and X. WU, “Enhancing the One-Dimensional SFR Thermal Stratification Model via Advanced Inverse Uncertainty Quantification Methods,” *Nucl. Technol.*, (2020); <https://doi.org/10.1080/00295450.2020.1805259>.
7. M. D. McKAY, R. J. BECKMAN, and W. J. CONOVER, “A Comparison of Three Methods for Selecting Values of Input Variables in the Analysis of Output from a Computer Code,” *Technometrics*, **42**, 1, 55 (1979); <https://doi.org/10.1080/00401706.2000.10485979>.
8. J. SCHNEIDER and M. ANDERSON, “Using Optical Fibers to Examine Thermal Mixing of Liquid Sodium in a Pool-Type Geometry,” *Int. J. Heat Mass Transfer*, **158**, 119968, (2020); <https://doi.org/10.1016/j.ijheatmasstransfer.2020.119968>.
9. L. H. SHIH et al., “Parameterization of Turbulent Fluxes and Scales Using Homogeneous Sheared Stably Stratified Turbulence Simulations,” *J. Fluid Mech.*, **525**, 193 (2005); <https://doi.org/10.1017/S0022112004002587>.
10. X. WU, T. KOZLOWSKI, and H. MEIDANI, “Kriging-Based Inverse Uncertainty Quantification of Nuclear Fuel Performance Code BISON Fission Gas Release Model Using Time Series Measurement Data,” *Reliab. Eng. Syst. Saf.*, **169**, 422 (2018); <https://doi.org/10.1016/j.res.2017.09.029>.
11. X. WU et al., “Inverse Uncertainty Quantification Using the Modular Bayesian Approach Based on Gaussian Process. Part 1: Theory,” *Nucl. Eng. Des.*, **335**, 339 (2018); <https://doi.org/10.1016/j.nucengdes.2018.06.004>.
12. J. K. FINK and L. LEIBOWITZ, “Thermodynamic and Transport Properties of Sodium Liquid and Vapor,” ANL/RE-95/2, Argonne National Laboratory (1995).
13. K. Q. YE, “Orthogonal Column Latin Hypercubes and Their Application in Computer Experiments,” *J. Am. Stat. Assoc.*, **93**, 444, 1430 (1998); <https://doi.org/10.1080/01621459.1998.10473803>.
14. J. C. HELTON and F. J. DAVIS, “Latin Hypercube Sampling and the Propagation of Uncertainty in Analyses of Complex Systems,” *Reliab. Eng. Syst. Saf.*, **81**, 1, 23 (2003); [https://doi.org/10.1016/S0951-8320\(03\)00058-9](https://doi.org/10.1016/S0951-8320(03)00058-9).
15. K. BURRAGE et al., “Populations of Models, Experimental Designs and Coverage of Parameter Space by Latin Hypercube and Orthogonal Sampling,” *Procedia Comput. Sci.*, **51**, 1762 (2015); <https://doi.org/10.1016/j.procs.2015.05.383>.
16. M. STEIN, “Large Sample Properties of Simulations Using Latin Hypercube Sampling,” *Technometrics*, **29**, 2, 143 (1987); <https://doi.org/10.1080/00401706.-1987.10488205>.
17. A. A. KHAN, L. LYE, and T. HUSAIN, “Latin Hypercube Sampling for Uncertainty Analysis in Multiphase Modelling,” *J. Environ. Eng. Sci.*, **7**, 6, 617 (2008); <https://doi.org/10.1139/S08-031>.
18. A. D. KIUREGHIAN and O. DITLEVSEN, “Aleatory or Epistemic? Does It Matter?,” *Struct. Saf.*, **31**, 2, 105 (2009); <https://doi.org/10.1016/j.strusafe.2008.06.020>.
19. J. R. TAYLOR, *An Introduction to Error Analysis*, University Science Books, Sausalito, California (1997).
20. C. LU and Z. WU, “Sensitivity Analysis of the 1-D SFR Thermal Stratification Model via Discrete Adjoint Sensitivity Method,” *Nucl. Eng. Des.*, **370**, 110920, online (2020); <https://doi.org/10.1016/j.nucengdes.2020.110920>.